Langmuir

Article

pubs.acs.org/Langmuir

Macro- versus Microscopic View on the Electrokinetics of a Water–Membrane Interface

Volker Knecht,*,† Benjamin Klasczyk,‡ and Rumiana Dimova

Theory & Bio-Systems, Max Planck Institute of Colloids and Interfaces, Science Park Golm, D-14424 Potsdam, Germany

Supporting Information

ABSTRACT: Electrophoresis is an experimental method widely used to study electrostatic properties of interfaces. Here, we question the validity of the macroscopic theory for the planar geometry by Helmholtz and Smoluchowski by considering a POPC bilayer in an aqueous solution with 500 mM NaCl, using molecular dynamics simulations. We find that POPC shows positive electrophoretic mobility due to adsorption of sodium ions at the lipid headgroups. The theory assumes that the region in which the water density undergoes a transition from the bulk value to zero (interfacial width) is small compared to the Debye screening length. This separation of length scale is not fullfilled in the present case. Hence, contrasting the theory, we observe that the surface is not sharply defined, continuum hydrodynamics is not applicable, the effective viscosity in the double layer is increased compared to the bulk, and the zeta potential is dominated by the dipole potential. Our results might have widespread implications for interpretation of electrokinetic studies in general.

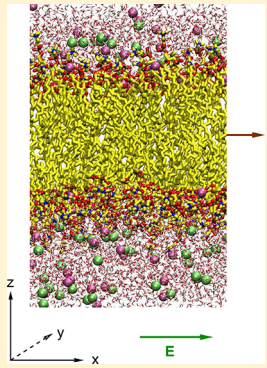

INTRODUCTION

An external electric field may induce migration of suspended particles or liquid flow through porous materials as first reported in 1809 by Reuss.[1] These electrokinetic phenomena are denoted as electrophoresis or electroosmosis, respectively. Both phenomena have in common that an electric field parallel to the interface between a liquid and another phase induces a relative drift between the liquid and the second phase parallel to the field, whereby the average drift velocity depends linearly on the field intensity. For electrophoresis, the drift velocity of the second phase relative to the liquid normalized by the field intensity is denoted as electrophoretic mobility. For electroosmosis, the average drift velocity of the liquid relative to a solid substrate is denoted as electroosmotic mobility.

These phenomena arise from an electric double layer at the interface between the phases. The first layer contains ionic species adsorbed at the surface by various chemical interactions. The second layer forms due to electrostatic attraction and electrically screens the first layer. The double layer contributes to a difference in electrostatic potential between the phases. Analytical theories propose relations between the electrophoretic or electroosmotic mobility and the electrostatic potential at the shear plane denoted as the zeta potential. Here, the case that the particle size or pore diameter, R, is large compared to the Debye screening length, $1/\kappa$, is described by the Helmholtz–Smoluchowski equation that has been used for a century.[2−4] Theories for arbitrary values of κR reproduce the Helmholtz-Smoluchowski equation if κR is large.[4−7] In particular, effects from curvature, surface conductivity, and polarization of the electric double layer are not present in this limit.[8] On the basis of these theories, electrophoresis, especially, is widely used to derive the zeta potential and other surface properties of colloidal particles.[4] A literature search on the topics zeta potential or electrokinetic potential yields 17585 articles and 437 reviews, thereof 1995 articles and 40 reviews have been published in 2012.

From the zeta potentials, the surface charge, σ_{ekin}, is deduced using the Gouy–Chapman theory. It is found, however, that σ_{ekin} is often much smaller than the estimate for the surface charge measured using other techniques. This discrepancy was solved in the past by postulating that a part of the counterions is dragged with the colloid undergoing electrophoretic motion due to the presence of a stagnant layer consisting of water and counterions that are immobilized on the surface of the colloid. The presence of a stagnant layer would imply that the shear plane resided about 0.3 nm above the surface. Molecular dynamics (MD) simulations suggested that the stagnant layer behaves like a two-dimensional gel with the shear viscosity for liquid flow parallel to the surface being enhanced by up to a factor of 2.[9] The position of the shear plane, though, was not determined in that study.

MD simulations are a powerful tool for understanding electrokinetic phenomena at a molecular level. Inversely, a molecular understanding of electrokinetic phenomena is indispensable for the validation of MD simulations in terms of ion-surface affinities by comparison to electrokinetic studies.

A general possible problem of the standard theory for electrokinetic phenomena is that it assumes an infinitely sharp transition in the liquid density between the liquid and the particle or the solid substrate. The latter implies a separation of length scales in that the width Δz of the region in which the water density shows the transition from the bulk value to zero is

Received: February 1, 2013
Revised: May 22, 2013
Published: May 22, 2013

small compared to the Debye screening length, λ_D. At aqueous interfaces, the water density undergoes a smooth transition on a length scale of $\Delta z \approx 1$ nm, as suggested by MD simulations.[10,11] On the other hand, the Debye length, λ_D, for a 1:1 electrolyte consisting of monovalent ions in aqueous solution is given by

$$\lambda_D = \left(\frac{\varepsilon_0 \varepsilon k_B T}{2ce^2}\right)^{1/2} \quad (1)$$

Here, ε_0 denotes the dielectric permittivity of vacuum, ε the relative permittivity of the solution, c the electrolyte concentration, k_B the Boltzmann constant, T the temperature, and e the proton charge. For water with $\varepsilon = 80$ at 300 K and $c \leq 1$ mM, $\lambda_D \geq 10$ nm such that $\Delta z \ll \lambda_D$ and the macroscopic description might be appropriate. In contrast, for $c = 10$ mM, $\lambda_D \approx 3$ nm such that λ_D and Δz are of the same order of magnitude and the theory may become inaccurate. For a physiological ion concentration of $c = 100$ mM, $\lambda_D \approx \Delta z$, such that the macroscopic description may break down and, instead, a molecular description might be necessary, which is not considered in the interpretation of electrophoresis experiments so far.

Important systems due to their biophysical relevance are phospholipid bilayers in aqueous solution. Therefore, to understand the importance of using a molecular rather than a continuum model to comprehend the electrokinetics of a lipid bilayer at ion concentrations close to physiological conditions, we have used MD simulations to study a palmitoyloleoylphosphatidylcholine (POPC) bilayer in an aqueous NaCl solution. The interaction of NaCl and POPC is of high biological relevance due to the abundance of POPC lipids in biological membranes and the presence of around 100 to 150 mM Na^+ and Cl^- ions in the extracellular medium. Though early electrophoresis experiments considering NaCl concentrations below 100 mM did not resolve the effect of NaCl on the electrophoretic mobilities of POPC liposomes,[12] more recent experiments considering ion concentrations of up to 500 mM indicated an excess adsorption of sodium ions.[13] Adsorption of NaCl at PC is also indicated by results from infrared[14] and fluorescence correlation spectroscopy,[10] as well as X-ray[15] and calorimetric experiments.[13] MD simulations suggest that sodium ions are adsorbed at the carbonyl oxygens of the POPC lipids (i.e., at the interface between the headgroup and the tail region of PC bilayers), whereas a diffuse layer with excess chloride ions form at the interface between the headgroups and the water.[10,16−23]

The interaction of PC with NaCl is found to lead to an increase in (i) the range of anisotropic water ordering close to a lipid bilayer, (ii) the membrane thickness, and (iii) the order parameters of the lipid tails, as well as a reduction in the area per lipid and the rate for self-diffusion of the lipids.[10] If a PC bilayer separates a water reservoir with containing NaCl and an ion-free reservoir, ion adsorption may induce a gradient in the electrostatic potential across the bilayer.[24] Na^+ ions bind more strongly to PC than to phosphatidylethanolamine (PE) lipids and more strongly to PC lipids than potassium ions.[18]

Previous MD studies have focused on analyzing the distribution of ions, lipids, and water, as well as the electrostatic potential profile across lipid bilayers, considering lipid bilayers in electrolyte solutions at equilibrium.[10,17−23,25−27] For the first time, using MD simulations, we explore the response of a POPC bilayer in aqueous NaCl solution to an external electric field parallel to the bilayer to test whether the assumptions underlying the Helmholtz-Smoluchowski equation are valid and whether the zeta potential is predicted correctly by this equation. Strikingly, we find that the shear plane resides within the headgroup region such that continuum hydrodynamics is not valid. The effective viscosity exceeds the bulk value, and the zeta potential estimated on the basis of individual point charges is an order of magnitude larger than estimated from the theory. This is due to the dipole potential, which is significant and even maximal at the shear plane.

CONTINUUM THEORY

Here, we introduce concepts from macroscopic theory relating electrophoretic mobilities to surface properties.[4] The corresponding relations will be questioned in the Results section by comparison to results from MD simulations. It is assumed that, above the shear plane, continuum hydrodynamics applies, and the viscosity is equal to the viscosity of the bulk solution, η. Hence, at steady state, the second derivative of the velocity profile along the interface normal, $v(z)$, is related to the applied electric field, E, and the charge density of mobile charges, $\rho_q(z)$, according to $\eta \partial^2 v(z)/\partial z^2 = -E\rho_q(z)$. Double integration of the charge density from a position $z \equiv z_b$ in the bulk, where $\rho_q(z) \approx 0$ to the shear plane $z \equiv z_s$ yields

$$\mu_E = -\frac{1}{\eta}\int_{z_b}^{z_s} dz' \int_{z_b}^{z'} dz'' \rho_q(z'') \quad (2)$$

It is further assumed that the dielectric permittivity in the shear layer is independent of z and equal to the value for the bulk solution, ε. Also, it is assumed that the dipole potential (i.e, the electrostatic potential arising from the anisotropic orientation of dipoles not related to dielectric response) is negligible. This leads to a relation between the zeta potential, ζ, and the electrokinetic mobility, μ_E, which reads

$$\mu_E = \frac{\varepsilon_0 \varepsilon \zeta}{\eta} \quad (3)$$

We emphasize that this equation is not a definition for the zeta potential as suggested in ref 28 but is derived based on the definition of the zeta potential to be the electrostatic potential at the shear plane. Smoluchowski obtained the same formula for the electrophoresis of a particle with a size large compared to the Debye screening length. If this separation of length scales is no longer valid, curvature effects must be taken into account.[4]

METHODS

Set-Up. A POPC bilayer in a sodium chloride solution in a rectangular box under periodic boundary conditions was studied using classical molecular dynamics simulations. The simulation system as shown in Figure 1 consisted of 128 lipid and $N_w = 5020$ water molecules, as well as $N_{NaCl} = 50$ NaCl ion pairs, corresponding to a salt concentration of $(N_{NaCl}/N_w)55.55$ M = 500 mM. A high ion concentration of approximately 500 mM was used in order to (i) induce significant electrophoretic activity of the POPC bilayer and (ii) ensure a small Debye screening length, allowing us to see bulk conditions within a reasonably small simulation box. The bilayer was parallel to the xy plane, and the initial configuration of the ion-free system with box dimensions of 6.4 nm ×6.4 nm ×7.8 nm was taken from our previous study.[19] The initial configuration of the system with ions was obtained by replacing water molecules by Na^+ or Cl^- ions at energetically favorable positions. The system with and without ions was simulated exposed to external electric fields, E_0, parallel to the x axis (see Figure 1) in the range of 0−0.2 V/nm, by applying an additional force, $F_i = q_i E_0$, to each atom with charge q_i. The field

dx.doi.org/10.1021/la400342m | Langmuir 2013, 29, 7939−7948

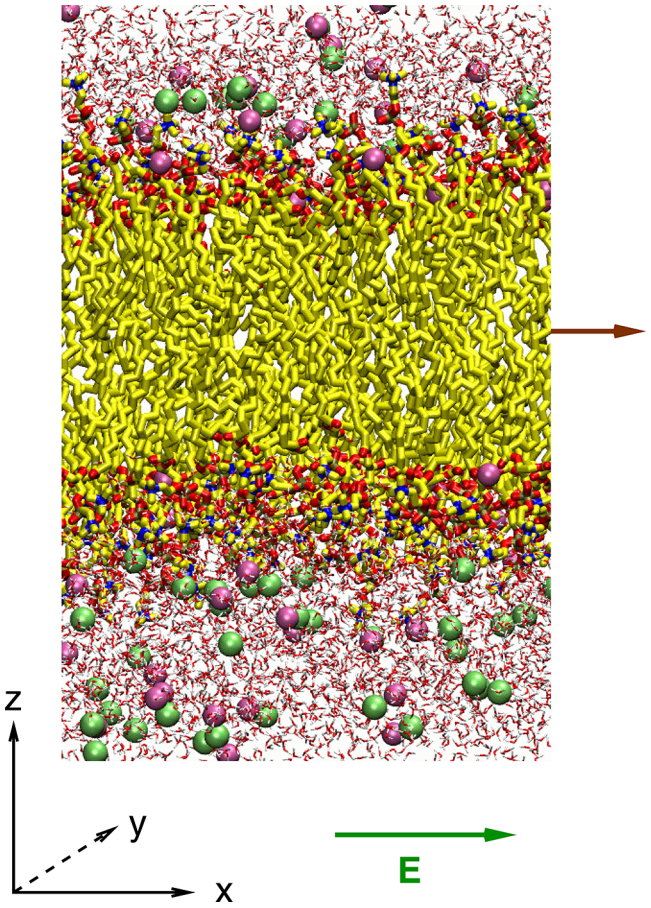

Figure 1. Simulated system, a POPC bilayer in water with ~500 mM NaCl, exposed to an effective electric field. The lipids are shown as thick and the water molecules as thin sticks, and the ions are depicted as spheres. Colors distinguish between carbons and hydrocarbon groups (yellow), oxygen (red), phosphate (brown), nitrogen (blue), and hydrogen atoms (white), as well as Na^+ (magenta), and Cl^- ions (green). The direction of the electric field (green arrow) and the field-induced migration of the membrane relative to the water (brown arrow) are shown.

strengths employed lie well in the linear response regime of water.[29] Each system was simulated for 100 ns for each field strength. Overall translational motion of the bilayer–water system in the x, y, and z direction was removed, whereas the motion of the bilayer with respect to the water was not removed. In order to study the distribution of ions in the bulk to check if the Debye length is meaningful at high salt concentrations, in addition, a cubic box with 4072 water molecules and 35 NaCl ion pairs, corresponding to an ion concentration of 470 mM, was simulated for 5 ns.

The force field for POPC lipids was taken from Berger et al.,[30] where hydrogens in hydrocarbon groups are treated implicitly using united atoms. The ions were described using GROMOS.[31] The water was treated using the rigid simple point charge (SPC) model.[32] This force field combination corresponds to a standard setup for MD simulations of lipid bilayers. The water molecules were kept rigid using the analytical constraint solver SETTLE,[33] and the lengths of covalent bonds in POPC were constrained using the LINear Constraint Solver (LINCS).[34] This enabled us to use a 2 fs time step for the integration of the equations of motion. The weak coupling technique by Berendsen et al. was employed to control the temperature or pressure with relaxation times of 0.1 and 1.0 ps, respectively.[35] For the bilayer systems, a pressure of 1 bar normal and lateral to the bilayer corresponding to a tension-free membrane were maintained by semi-isotropic scaling of the simulation box. For the bulk solution, a pressure of 1 bar was maintained via isotropic scaling of the simulation box.

The setup, in particular, the water model and the thermostat, were chosen such as to be consistent with previous simulation studies of the interaction of NaCl with PC bilayers at equilibrium.[10,18,20] We especially chose the SPC and not the related SPC/E model for the water, though the latter more accurately reproduces bulk properties, because, inversely, the SPC model appears to be more accurate at interfaces as explained in the Supporting Information.

The standard for simulations using the Berger force field for the lipids is to truncate the Lennard–Jones (LJ) interactions at 1 nm without further modification of the original LJ potential.[30] However, it has been shown recently that the usage of plain cutoff truncation, implying a discontinuous force distance relationship, may lead to spurious electrophoretic activity in the absence of surface charge. The effect decreases with increasing cutoff distance and vanishes if the interactions are smoothed by further modification of the LJ interactions.[36] Thus, in the present work the LJ interactions were smoothed by switching them from finite to zero in an appropriate distance range, considering the original cutoff distance used for plain cutoff truncation. In brief, LJ interactions were treated unchanged for interatomic distances r with $0 < r < r_1 = 0.7$ nm; for $r_1 < r < r_c = 1.1$ nm, a third degree polynomial $S(r)$ denoted as a switch function was added to the force such that the modified force and its derivative were continuous at $r = r_1$ and $r = r_c$. Full electrostatic interactions were evaluated using the particle mesh Ewald (PME) technique,[37] with a 1 nm cutoff for direct space, a 0.12 nm grid spacing, and an interpolation order of 4. Nonbonded neighbor lists were updated every 5 steps. The parameters for PME used correspond to standard settings employed in MD simulations. All simulations were performed using GROMACS, version 3.[38] Configurations were saved every 10 ps for further analysis.

Analysis. Analyses of the systems at equilibrium or at steady states were performed, omitting the initial 20 ns for relaxation. Here, we followed the protocol used in previous simulations of related systems where excellent agreement of simulated and experimental values for the rates of lipid self-diffusion at different ion concentrations was obtained.[10] If not stated otherwise, standard errors were evaluated from block averages dividing the trajectories into four fragments.[39] In order to analyze the electrophoretic motion, the position of the center of mass of the bilayer, relative to the center of mass of the water in field direction x and (as a control) normal to the field directions y and z, was studied as a function of time. Hence, migration rates $v_{CoM} \equiv \Delta x/\Delta t$ (for y and z directions, accordingly) were determined. The choice of the relaxation period was validated by comparing the migration rates at $E_0 = 0.2$ V/nm obtained by skipping the initial 20 or 60 ns; the corresponding migration rates agreed within the statistical error, suggesting that the relaxation period chosen was appropriate. Corresponding electrophoretic mobilities, $\mu_{E,CoM}$, were obtained from fitting the function $v = \mu_{E,CoM}E_{app}$ to the data, with the effective electric field, E_{app}, taken equal to the electric field in the water bulk. The latter was determined from[40]

$$E_{app} = \frac{np}{(\varepsilon - 1)\varepsilon_0} \tag{4}$$

Here, p denotes the average dipole moment of a water molecule in the field direction in the water phase at least 1 nm away from the position at which the water density equals half the density in the bulk. Furthermore, ε_0 is the permittivity of vacuum, and $n = 33/\text{nm}^3$ is the bulk number density of the water molecules. Note that the concentration of pure water in water is 55.55 M, corresponding to 33.5 water molecules per nm^3. In consideration of the fact that for ~500 M NaCl about 1 M of water is replaced by ions (one water molecule per cation and anion), the concentration of water in the aqueous solution simulated is expected to be about 54.55 M, corresponding to 32.9 water molecules per nm^3. Thus, the water density is in good agreement with what is expected from experimental values. This is plausible, as the SPC water model is actually parametrized to match the density (and heat of vaporization) of bulk water at the temperature and pressure considered in our

dx.doi.org/10.1021/la400342m | Langmuir 2013, 29, 7939–7948

simulations.[32] The dielectric permittivity chosen was that for SPC water, $\varepsilon = 61 \equiv \varepsilon_{SPC}$.[41]

The spatial flow pattern was studied by comparing the average velocity, v_{loc}, of atoms with the number of atoms per unit volume for selected groups along the distance z normal to the interface at an effective field of 0.17 V/nm. The flow profile $v_{loc}(z)$ was evaluated by choosing a bin width of 0.01 nm. The number of heavy atoms per unit volume for the ions, the water, and the lipids along the z axis were determined by dividing the z range into 1200 bins. The charge density, $\rho_q(z)$, was obtained from

$$\rho_q(z) = \langle \sum_{i;|z_i - z| < \Delta z/2} q_i/\Delta V(z) \rangle \quad (5)$$

by dividing the z range into 600 bins. Here, z_i denotes the position of atom i normal to the interface, q_i is the partial charge of atom i, $\Delta V(z)$ denotes the volume element associated with the interval $[z_i - \Delta z/2, z_i + \Delta z/2]$, and $\langle ... \rangle$ indicates time averaging.

Electrostatic Potential. The estimate for the electrostatic potential difference across an interface in a molecular system depends on the convention for summing up the contributions of polar molecules to the electrostatic potential, which can be done either on the basis of point charges within entire molecules (M scheme) or on the basis of individual point charges (P scheme). On the basis of an analysis of liquids composed of spherical solvent molecules (represented by a classical solvent model with a single van der Waals interaction site), Kastenholz and Hünenberger concluded that the M scheme is the appropriate way of calculating the electrostatic potential.[42] However, it is unclear whether this conclusion can be extended to systems with larger and more complex molecules, such as phospholipids. Hence, in the current paper, we use the P scheme, which is the most commonly employed method for evaluating electrostatic potential profiles along lipid bilayers. Therefore, the electrostatic potential $\Phi(z)$ with respect to bulk water was determined from

$$\Phi(z) = \frac{1}{\varepsilon_0} \int_z^{z_{max}} \int_{z_{max}}^{z'} \rho_q(z'')dz'' \quad (6)$$

Here z_{max} resides in the bulk water. The average velocity $v_{loc}(z)$ of all atoms from lipids, water molecules, and ions in slices of thickness of 0.005 nm at position z normal to the bilayer was determined using a 0.005 nm bin width with subsequent smoothing by running averages over 100 bins.

The origin of the z axis, $z = 0$, was set to the position where the water density equaled half the bulk density, with $z < 0$ corresponding to the membrane and $z > 0$ to the water side of the origin. This was done for the analysis of both leaflets. From $v(z)$, the position of the shear plane, z_s, was determined using the condition that $v_{loc}(z) = v_m$ for $z < z_s$ and $v_{loc}(z) < v_m$ for $z > z_s$, with v_m denoting the average drift velocity of the membrane. From an upper and lower bound for the left leaflet, $z_{s,1}$ and $z_{s,2}$, accordingly, as well as an upper and lower bound for the right leaflet, $z_{s,3}$ and $z_{s,4}$, respectively, the average and standard error were computed.

The effective zeta potential, ζ, was determined from the corresponding values of the electrostatic potential $\Phi(z_{s,i})$, with $i = 1, 2, 3, 4$. The average of these values and the corresponding standard error yielded the zeta potential and its statistical error.

The distribution of NaCl ions in the bulk system was evaluated by determining the Na−Cl pair correlation function $g_{+-}(r)$ and, hence, the underlying potential of mean force (PMF), $G(r)$, using

$$G(r) = -k_B T \ln g(r) \quad (7)$$

where T denotes the absolute temperature and k_B Boltzmann's constant. This was compared to the effective potential between monovalent cations and anions predicted from the Debye−Hückel theory according to

$$G_{DH}(r) = \frac{e^2}{4\pi\varepsilon_0\varepsilon r} e^{-r/\lambda_D} \quad (8)$$

with λ_D denoting the Debye screening length as given by eq 1. Here, ε was set to the value for SPC water and the concentration c in eq 1 to 470 mM.

RESULTS

Figure 2 shows the migration rates, v, of the center of mass of the POPC bilayer relative to the center of mass of the water in the field direction as a function of the field intensity, E. The figure shows the behavior in the absence as well as in the presence of ~500 mM NaCl. In the absence of ions (Figure 2a, open symbols), no significant drift of the POPC bilayers in the field direction is detected. Experimentally, the electrophoretic mobilities of PC vesicles in the absence of salt depend on the pH being negative above and positive below pH 4, the isoelectric point (iep).[43] Our system thus appears to mimic experimental conditions at the iep.

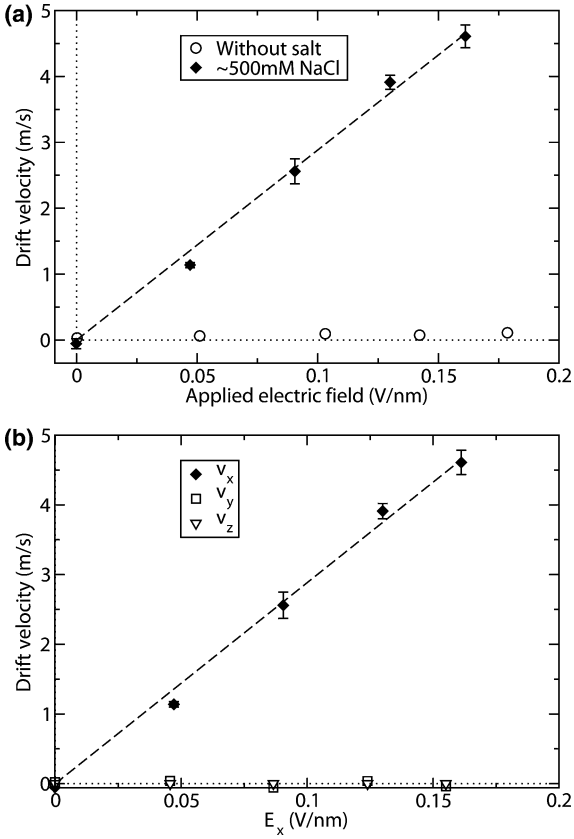

Figure 2. Electrophoretic drift of the center of mass (CoM) of a lipid bilayer in the xy plane with respect to the CoM of the water in the presence of an applied electric field (E_x, 0, 0) (a) in the x direction in the absence (open symbols) and presence (filled symbols) of ions, as well as (b) in x (filled symbols) and the y or z direction (open symbols) in the presence of ions.

As shown in Figure 2, addition of NaCl in our simulations leads to a drift of the POPC bilayer parallel [(a) and (b), filled symbols] but not normal to the field [(b), open symbols]. We note that very high electric field intensities are needed to distinguish electrophoretic drift from diffusion on the limited time and length scales of MD simulations.[44] Macroscopic electrophoresis experiments aimed to infer zeta potentials typically use much lower field intensities on the order of 1×10^{-6} V/nm.[45] At such field intensities, though, nonlinear electrophoresis has been observed for double-stranded DNA

dx.doi.org/10.1021/la400342m | Langmuir 2013, 29, 7939−7948

molecules in gels (i.e., molecules which were large compared to their persistence length and migrated through especially highly viscous media). Here, the molecules deformed and aligned with the field, leading to nonlinear effects. The nonlinear effect decreased with decreasing size of the molecules.[46] Inversely, MD simulations of the electrophoresis of single-stranded RNA oligomers in aqueous solution at field intensities comparable to the ones employed in the present work yielded a linear dependence of migration rates on the field intensities.[44] Experimentally, electric fields exceeding 0.01 V/nm were employed in microsecond electrophoresis studies of photoreaction intermediates, and again the migration rates were found to be independent of the field intensities.[47] Finally, in the present work the migration rates of the lipid bilayer are found to be linear in the field intensities, indicating that nonlinear effects are not significant for this system. Hence, we observe linear electrophoresis and normalizing the migration rates by the field intensities allows for extrapolation to conditions of low field intensities typically used in electrophoresis experiments on lipid vesicles. As the migration is in the field direction, the POPC bilayer shows a positive electrophoretic mobility. Also, experimentally it was observed that addition of NaCl to aqueous solutions containing POPC vesicles renders the electrophoretic mobilities of the vesicles more positive.[13]

Figure 3a shows the number of heavy atoms per unit volume for the lipids, the water, as well as the Na^+ and the Cl^- ions, along the position z normal to the bilayer. As seen from the densities of the lipids and the water, the surface is not sharply defined in contrast to the theoretical assumption but in agreement with findings from previous MD studies.[10,20] We define the origin $z = 0$ as the position at which the water density equals half the bulk density (Gibbs dividing surface). A high peak for Na^+ ions is centered at $z = -0.51$ nm and coincides with the peak from the carbonyl oxygens. This is consistent with results from previous MD simulations and IR spectroscopy, which indicate that the Na^+ ions bind to the carbonyl oxygens, leading to a partial dehydration of the lipid headgroups.[10,14] Isothermal titration calorimetry indicates that the binding of Na^+ ions to PC bilayers is entropically driven, and the entropy gain is attributed to the gain in water entropy due to the partial release of hydration water.[13] In the aqueous phase close to the membrane, Na^+ is depleted and Cl^- enriched, while their concentration is equal to the bulk value of 470 mM for $z > 1.76$ nm $\equiv z_b$.

Figure 3b shows the average drift velocity v along z for an external electric field of $E = 0.17$ V/nm. The electrophoretic mobility μ_E of the bilayer was determined from $\mu_E = v/E$, with $v = 6.16$ ($\pm$0.45) m/s denoting the average velocity for $z < zs$ with respect to the bulk ($z > z_b$), yielding $\mu_{E,MD} = 40.28 \times 10^{-5}$ cm^2/(V s). In our simulations, the absolute electrophoretic mobility is equal to the change in mobility upon addition of NaCl, $\mu_{E,MD} = \Delta\mu_{E,MD}$. Experimentally, addition of 500 mM NaCl to POPC vesicles in aqueous solution changed the electrophoretic mobilities by $\Delta\mu_{E,exp} = 3.98 \pm 1.51 \times 10^{-5}$ cm^2/(V s).[13] Hence, $\mu_{E,MD} = 10\Delta\mu_{E,exp}$, indicating force field issues that have been discussed recently and that appear to apply to all force fields that have so far been used to study the interaction of NaCl with PC bilayers.[48]

The problem emerging here is circular. To understand the interaction of ions with lipid bilayers from the electrophoretic mobilities requires an electrokinetics theory. Such a theory should be validated at the molecular level, using MD simulations. MD simulations appear not to be accurate in terms of ion–lipid affinities. However, from comparing μ_E, it is not clear if the discrepancy in terms of μ_E arises from an overestimation of the Na^+–PC or an underestimation of the Cl^-–PC affinity, or a combination of both.[48] A first step toward resolving this issue is to understand zeta potentials at given electrophoretic mobilities, which is possible using the force field employed here.

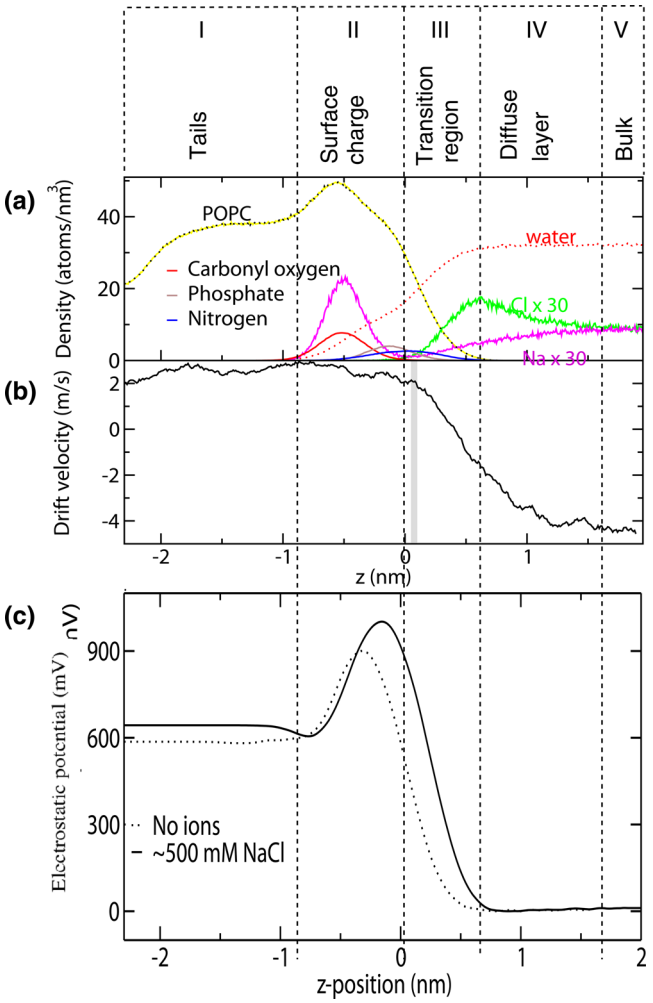

Figure 3. (a) Number of selected groups of heavy atoms per unit volume (partial densities) and (b) local drift velocity, both at an external electric field of 0.17 V/nm parallel to the bilayer across the membrane–water interface. The partial densities of the ions are scaled by a factor of 30. In (b), the gray region marks the location of the shear plane.

A challenge in our validation of the theory is to distinguish between (i) possible force field inaccuracies in terms of material parameters and ion–lipid affinities on the one hand and (ii) inconsistencies of the theory on the other hand, the latter being our main interest. Not to mix up (ii) with (i), we test the validity of the HS equation by using the viscosity and the dielectric permittivity set to the corresponding values of SPC water, $\eta = 4.3 \times 10^{-4}$ kg m^{-1} s^{-1}[49] and $\varepsilon = 61$.[41] These values differ from the experimental ones, as the SPC model has been fitted against other observables (density and heat of vaporization), and with a simple model like SPC, one cannot reproduce all experimental values with the same accuracy. From the electrophoretic mobilities determined here, the HS equation yields $\zeta_{HS} = 28.2$ ($\pm$2.1) mV.

dx.doi.org/10.1021/la400342m | Langmuir 2013, 29, 7939–7948

Hydrodynamic Aspects. In order to validate the theory, we evaluated the zeta potential also directly from our simulations. To this aim, the position of the shear plane, z_s, was determined from the flow profile observed in the external electric field (and not from the distribution of lipids and water normal to the bilayer).

Continuum Hydrodynamics Invalid. In accordance with the derivation of the HS equation, the shear plane location, z_s, must have the properties $v(z_s) = v_m$ and $v(z) < v_m$ for $z > z_s$, where v_m denotes the average drift velocity of the membrane. This property applies to the kink in $v(z)$ located at $z_s = 0.166$ ($\pm$0.056) nm (the uncertainty being indicated as a gray-shaded area in Figure 3b; the fact that the area is very narrow indicates that the position of the shear plane is well-defined).

Experimental studies of lipid membranes located the shear plane 0 to 0.2 nm above the surface.[12] This was based on the assumption that the position of the surface itself is defined by an accuracy of about 0.2 nm. However, as seen in Figure 3, this is not the case. The distance over which the water density undergoes a transition from the bulk value to zero is about 1 nm. Thus, the position of the surface is not well-defined and cannot be used as a meaningful reference for the position of the shear plane. The latter, nevertheless, is well-defined from the flow profile. In this respect, our conclusions are new (i.e., different from the traditional view).

Further differences with the traditional view are that (i) the shear plane resides between the Na^+ and the Cl^- layer, such that the counterions are not dragged with the bilayer, and (ii) the shear plane resides in the headgroup region where continuum hydrodynamics, used in the derivation of the HS equation, is not applicable in a rigorous sense. Whereas continuum hydrodynamics implies that at steady state all atoms of a plane normal to the z axis with $z > z_s$ move with the same velocity, in our system, only the water molecules in the headgroup region can flow, whereas the atoms of lipid molecules are obviously stationary relative to the bilayer. Hence, an idealized shear plane as assumed in continuum hydrodynamics does not exist on a molecular level, nor does a zeta potential in the original sense.

On a larger scale than studied here (i.e., replacing lipid headgroups by polymers), hindrance of water molecules by macromolecules associated with a suspended particle has been considered in self-consistent mean-field calculations for the electrophoresis of liposomes with coatings of terminally anchored poly(ethylene glycol) (PEG) polymers. There, the hydrodynamic size (Stokes radius) of the statistical PEG segments, a_s, was treated as an adjustable parameter. Fitting this model to the experimental data yielded an unphysically small value of $a_s = 0.0175$ nm (corresponding to a subatomic length scale), which indicated limitations of this mean-field hydrodynamic model,[50] highlighting the need for a more accurate description by molecular simulations.

The viscosity can be calculated from fluctuations at equilibrium[9] or, alternatively, from the response of the system to external shear in nonequilibrium simulations, as performed here. In accordance with eq 2, the effective viscosity η_{eff} in the Cl^- layer where $\rho_{q,ions} < 0$ leading to electrophoretic mobility μ_E is

$$\eta_{eff} = -\frac{1}{\mu_E}\int_{z_b}^{z_s} dz' \int_{z_b}^{z'} dz'' \rho_{q,ions}(z'') \tag{9}$$

Here, $\rho_q(z)$ is given by

$$\rho_{q,ions}(z) = +en_+(z) - en_-(z) \tag{10}$$

with $n_+(z)$ and $n_-(z)$ denoting the local concentration of Na^+ and Cl^- ions, respectively, and e the proton charge. The standard electrokinetics theory assumes that above the shear plane, the viscosity is equal to the bulk viscosity, $\eta_{eff} = \eta_{bulk}$. However, we find $\eta_{eff} = 9.28\ (\pm 0.75) \times 10^{-4}$ kg m^{-1} s^{-1} = 2.16 ($\pm$0.17)η_{SPC}.[49] Thus, the effective viscosity is 2-fold larger than the viscosity of the bulk water. Similarly, it was found that the shear viscosity of the first solvent layer on a smooth solid was found to be up to 2 orders of magnitude larger than the bulk viscosity.[9] However, in that work, it was assumed that this layer is below (on the solid side of) the shear plane. Our work, on the other hand, shows that the viscosity is (also) enhanced above (on the solution side of) the shear plane.

In accordance with the Einstein relation, the viscosity η is inversely proportional to the diffusion constant of particles, D, $\eta \propto 1/D$. The effective viscosity at the water−membrane interface found here may thus be related to diffusion constants for water close to membranes found previously. In particular, η_{eff} should be related to the value for the diffusion of water parallel to the interface, $D_\parallel$. A significant reduction of $D_\parallel$ has been detected from pulsed field gradient-spin echo NMR studies of water diffusion in aligned eggPC bilayer stacks compared to bulk water.[51] At 20 water molecules per lipid, the average value of $D_\parallel$ was a factor of 5.8 lower than D for bulk water.[51] MD simulations show that $D_\parallel$ in POPC at approximately 27 water molecules per lipid, depending on the distance of the water from the membrane center, varies by a factor of 10.[52] In our case, η_{eff} is presumably determined by the viscosity in the region around the peak in the choline distribution, as the size of the excess charge density $\rho_q(z)$ above the shear plane is maximal here. This position is at z = 0.6 nm. Rog et al. found that $D_\parallel$ for water molecules not closer than 0.7 nm away from any membrane atom, $D_\parallel \approx D_{bulk}/1.7$ and, hence, $\eta_\parallel = 1.7\eta$,[49] close to our result.

Effective Viscosity Higher than in Bulk Liquid. In order to map the continuum model to the molecular description, we define the plane $z = z_s$, characterized by the inequalities in the previous paragraph, as an effective shear plane and the electrostatic potential at z_s as an effective zeta potential. For slices at distance z with $z > z_s$ with lipid headgroups present, only the water and not the lipids show flow has two consequences: first, as $v(z)$ is obtained by averaging over the water and the lipids, $v(z)$ relative to the bulk water is smaller than the average velocity of the water molecules; second, the average velocity of the water molecules will be smaller than expected from continuum hydrodynamics for the case that the viscosity were equal to the value in the bulk liquid. This is because the motion of the water molecules is hindered by the presence of the lipid headgroups.

Zeta Potential. Required to determine the effective zeta potential, ζ, from the simulations is the profile of the electrostatic potential, Φ, along the z direction. In accordance with the first Maxwell equation, this electrostatic potential profile can be obtained from a double integration of the charge profile arising from the ions, the lipids, and the water. The resulting profile is shown in Figure 4. For the zeta potential, we find that $\zeta \equiv \Phi(z_s) = 705\ (\pm 89)$ mV = 25.0 ($\pm$1.8)ζ_{HS}, which exceeds the theoretical value by an order of magnitude.

Dominance of Dipole Potential. The large deviation of ζ_{HS} from ζ not only arises from an incorrect assumption concerning the effective viscosity but also from the assumption

dx.doi.org/10.1021/la400342m | Langmuir 2013, 29, 7939−7948

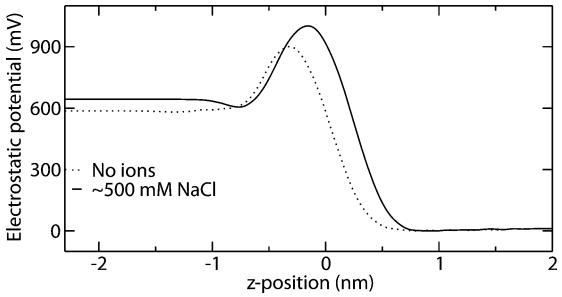

Figure 4. Electrostatic potential across the membrane−water interface in the absence and presence of NaCl.

that at the shear plane, the dipole potential is negligible. The dipole potential is the contribution to the electrostatic potential not corresponding to dielectric screening and is present even in the absence of ions. The electrostatic potential profile in the absence of ions, $\Phi_{dip}(z)$, is shown in Figure 4. We find that in the absence of ions, and hence in the absence of surface charge, the zeta potential is $\zeta_{dip} = \Phi_{dip}(z_s) \approx 563\ (\pm 60)$ mV.

As shown in Figure 5, the contribution of the lipids to the potential in our simulations is negative but overcompensated by

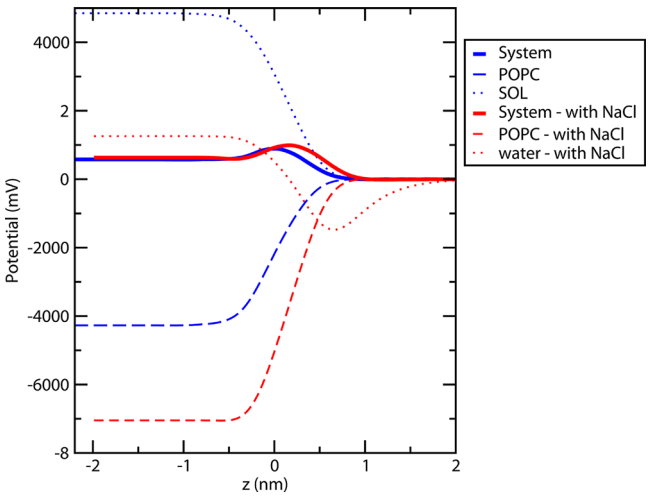

Figure 5. Electrostatic potential across the membrane−water interface (solid lines) in the absence (blue) and presence of ions (red), as well as respective contributions from the lipids (dashed lines) and the water (dotted lines), at an external electric field of 0.17 V/nm parallel to the bilayer.

the water contribution indicating anisotropic water dipole orientation, as observed from earlier simulations of lipid bilayers.[10] Spontaneous anisotropic orientation of water molecules at the interface to a low dielectric medium is also observed for other systems such as water−oil[53] or water−vapor interfaces.[54−56] For symmetry reasons, such preferred dipole orientation would not occur if water molecules were solely dipoles. Due to the presence of a quadrupole moment on the water molecules and the gradient in dielectric permittivity, this symmetry is broken, giving rise to an average net orientation of the dipole moment normal to the interface.[57,58]

The dipole potential, Φ_{dip}, is thus expected to scale with $c = p\varepsilon_w/\varepsilon_m$, where p is the dipole moment of the interfacial water molecules, p, and ε_w or ε_m are the dielectric constants of the water or the membrane, respectively. In the following, we scale the dipole potential in order to correct for known force field dependencies of the dipole moment of water molecules, as well as the dielectric permittivities of water and the membrane interior. In this scaling, the experimental or theoretically estimated values are compared with the values for the force field chosen. Experimentally, $\varepsilon_{w,exp} = 80$ at 293 K, and theoretical calculations yield $\varepsilon_m = 2.53$. The dipole moment of the interfacial water molecules, p, is expected to reside in the range of the value for the bulk water $p_{liq} = 2.95$ D and that for the gas phase, $p_{gas} = 1.85$ D. The value for the liquid and the gas phase differ due to the polarizability of the water molecules. The SPC water model used here is a nonpolarizable model, which implicitly includes the effect of the polarizability by an increased permanent dipole moment of the water molecules of $p_{SPC} = 2.27$ D. For the united atom model used here, the dielectric constant of the membrane interior is $\varepsilon_{m,MD} = 1$. A lower bound for the experimental dipole potential $\Phi_{dip,exp}$ may therefore be estimated via

$$\Phi_{dip,exp} \leq \Phi_{dip,MD} \frac{p_{gas}\varepsilon_{w,exp}/\varepsilon_m}{p_{SPC}\varepsilon_{w,SPC}/\varepsilon_{m,MD}} \tag{11}$$

yielding $\Phi_{dip,exp} \leq 245$ mV. This is close to the value 222.7 (± 9.8) mV for PC bilayers in the absence of salt measured experimentally using voltage-sensitive dyes.[43] The presence of the ions leads to a relatively small change in the total dipole potential but strongly alters the individual contributions by the water and the lipids, as observed earlier.[10] Whereas the presence of the ions reduces the contribution of the lipids, it enhances that of the water molecules.

Interpolation between High and Low Salt Conditions. The standard electrokinetics theory assumes that the interfacial width Δz is small compared to the thickness of the double layer given by the Debye screening length, λ (i.e., $\xi \equiv \Delta z/\lambda \ll 1$). For a 1:1 electrolyte with the bulk concentration, c, $\lambda \propto c^{-1/2}$, such that $\xi \propto c^{1/2}$. In the asymptotic limit of small c, $\xi \ll 1$ will hold, and the theory is valid. For increasing c, ξ will become comparable to 1, and deviations will occur. The case of a high ion concentration, $c \approx 470$ mM, has been studied here for technical reasons. The ion concentrations used are above ion concentrations in physiological bulk solutions. They are, however, comparable to the ionic conditions close to charged membranes where the effective ion concentrations are enhanced due to the enrichment in counterions.

Anyway, it would be intriguing to extrapolate our results to lower ion concentrations. Fortunately, we do not have to extrapolate but we can interpolate between the high ion concentration considered here and the limit of dilute conditions treated by the theory. This shall be done here by focusing on the effective viscosity η_{eff}. It is reasonable to assume that the deviation of η_{eff} from the bulk value η scales as $(\eta_{eff} - \eta)/\eta \propto \xi \propto c^{1/2}$, yielding

$$s_\eta(c) \equiv \frac{\eta_{eff}}{\eta} = 1 + \alpha_\eta c^{1/2} \tag{12}$$

which leads to $\alpha_\eta = 0.0535\ (\pm 0.0078)$ mM$^{-1/2}$. To interpolate to physiological conditions, we note that the intracellular medium of a human cell contains 100−150 mM K^+ ions and the extracellular medium 145 mM Na^+ ions. Equation 12 yields $s(100\text{ mM}) = 1.535\ (\pm 0.078)$ and $s(150\text{ mM}) = 1.655\ (\pm 0.096)$, which still are significant deviations from the theory ($s = 1$).

Our interpolation is based on the assumption that the Debye length λ is a meaningful concept at the high ion concentrations

dx.doi.org/10.1021/la400342m | Langmuir 2013, 29, 7939−7948

considered here. To check if this is indeed true, we consider that, within the Debye–Hückel theory, λ is the decay length for the effective interaction between ions in an electrolyte solution according to

$$V_{TH}(r) = \frac{q_1 q_2}{\varepsilon_0 \varepsilon r} e^{-r/\lambda} \quad (13)$$

Figure 6 shows $V_{TH}(r)$ for $q_1 = e$ and $q_2 = -e$, with e denoting the elementary charge. Here, λ was determined from eq 1 with

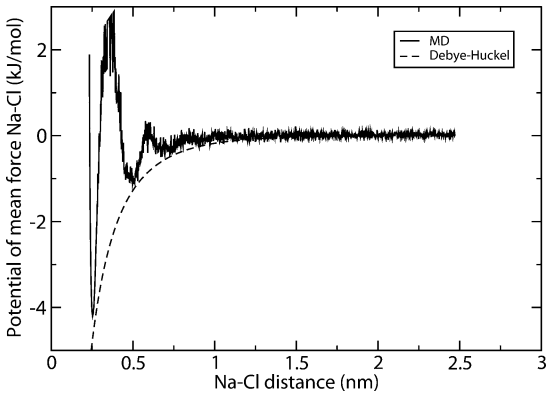

Figure 6. Potential of mean force along the distance between a Na^+ and a Cl^- ion in an aqueous solution with 470 mM NaCl from an MD simulation (solid line) vs prediction from the Debye–Hückel theory (dashed line).

c = 470 mM and $\varepsilon = \varepsilon_{SPC}$. For comparison, the effective interaction between Na^+ and Cl^- ions in an aqueous solution with 470 mM NaCl from an MD simulation, $V_{MD}(r)$ is shown. Here, $V_{MD}(r) = k_B T \ln g(r)$, where $g(r)$ denotes the pair correlation function between Na^+ and Cl^- ions. Whereas $V_{TH}(r)$ is monotonous, $V_{MD}(r)$ displays a damped oscillation with pronounced maxima at 0.35 nm, 0.59 nm, and 0.83 nm, as well as a minima at 0.25 nm, 0.51 nm, 0.70 nm, and 0.91 nm, within the interaction range, showing that molecular details are important to get the precise effective interaction. Interestingly, though, the minima lie exactly on the theoretical curve derived from λ_D without fitting, demonstrating the relevance of the Debye length, even at the ion concentration chosen here. This gives confidence that the interpolation formula eq 12 based on the relation between λ_D and c is appropriate and that the results of our work have implications also for lower, physiologically, and experimentally more relevant ion concentrations.

Refining Interpretation of Experimental Electrophoretic Mobilities. Our work facilitates a refined interpretation of experimental electrophoretic mobilities, μ_E, by modifying the HS equation. First, the bulk viscosity η should be replaced by the effective viscosity given by eq 12. Second, μ_E does not probe the absolute zeta potential, ζ, as the dipole potential is not associated with surface charge and therefore not with electrophoretic motion. Rather, μ_E probes the contribution, $\Delta\zeta$, of the surface charges to the zeta potential. In the case of our system, $\Delta\zeta$ is given by $\Delta\zeta = \zeta - \zeta_{dip}$, where ζ_{dip} denotes the zeta potential in the limit of the zero surface charge, as given by

Table 1. Surface-Charge-Induced Zeta Potentials from Continuum Theory, $\Delta\zeta_{TH}$, and Refined Estimates from eq 15, $\Delta\zeta$, for Several Studies from the Literature.[a]

reference	salt	lipid composition	$\Delta\zeta_{TH}$ (mV)	$\Delta\zeta$ (mV)
59	KNO_3	DMPC	−17	−26.0962
12	LiCl	PS	−59.5 (±1.5)	−91.34 (±0.12)
12	NaCl	PS	−62.0 (±1.0)	−95.17 (±0.078)
12	NaH_4Cl	PS	−72.0 (±1.5)	−110.52 (±0.12)
12	KCl	PS	−73.0 (±1.5)	−112.06 (±0.12)
12	RbCl	PS	−76.5 (±1.0)	−117.433 (±0.078)
12	CsCl	PS	−79.5 (±2.0)	−122.04 (±0.16)
12	LiCl	PG	−60.0 (±1.0)	−92.104 (±0.078)
12	NaCl	PG	−63.5 (±1.0)	−97.477 (±0.078)
12	NaH_4Cl	PG	−70.0 (±0.5)	−107.455 (±0.039)
12	KCl	PG	−72.5 (±0.5)	−111.293 (±0.039)
12	RbCl	PG	−76.0 (±1.0)	−116.665 (±0.078)
12	CsCl	PG	−79.0 (±1.0)	−121.271 (±0.078)
12	LiCl	PI	−49.0 (±1.0)	−75.218 (±0.078)
12	NaCl	PI	−45.0 (±1.0)	−69.078 (±0.078)
12	NaH_4Cl	PI	−49.0 (±1.0)	−75.218 (±0.078)
12	KCl	PI	−47.5 (±1.0)	−72.916 (±0.078)
12	RbCl	PI	−50.5 (±1.0)	−77.521 (±0.078)
12	CsCl	PI	−51.5 (±1.0)	−79.056 (±0.078)
12	LiCl	PA	−65.0 (±2.5)	−99.78 (±0.20)
12	NaCl	PA	−69.0 (±3.5)	−105.92 (±0.27)
12	NaH_4Cl	PA	−81.0 (±5.0)	−124.34 (±0.39)
12	KCl	PA	−83.5 (±1.0)	−128.178 (±0.078)
12	RbCl	PA	−88.5 (±1.0)	−135.854 (±0.078)
12	CsCl	PA	−90.5 (±1.5)	−138.92 (±0.12)
60	NaCl	30:70 (molar) PG/PC	−40	−61.4028

[a] The ion concentration considered for the systems shown was 100 mM. Lipids investigated in ref 12 were bovine brain phosphatidylserine (PS), egg phosphatidylglycerol (PG), bovine phosphatidylinositol (PI), and bovine phosphatic acid (PA), and the buffer used was 10^{-4} M EDTA for PS and 5 × 10^{-4} M EDTA for PG, PI, and PA.

dx.doi.org/10.1021/la400342m | Langmuir 2013, 29, 7939–7948

the value for a POPC bilayer in the absence of salt. The theory assumes $\zeta_{dip,TH} = 0$ and, hence, $\Delta\zeta_{dip,TH} = \zeta_{TH}$.

The modified HS equation thus reads

$$\mu_E = \frac{\varepsilon_0 \varepsilon \Delta\zeta}{\eta_{eff}} \quad (14)$$

Solving for $\Delta\zeta$ and denoting the estimate for the zeta potential from continuum theory by ζ_{HS} yields

$$\Delta\zeta = \Delta\zeta_{TH} s(c) \quad (15)$$

with $s(c)$ given by eq 12. Our estimates in the previous section thus suggest that for an aqueous solution with 100 mM of a 1:1 electrolyte, $|\Delta\zeta_{TH}|$ underestimates $|\Delta\zeta|$ by 50%. Table 1 shows relative zeta potentials for vesicles composed of various negatively charged lipids in aqueous 100 mM alkali metal chloride or NaH_4Cl solutions, comparing $\Delta\zeta_{TH}$ from the literature with our refined estimate $\Delta\zeta$ via eq 15.

CONCLUSION

In our MD simulations a POPC bilayer in aqueous solution with 470 mM NaCl shows positive electrophoretic mobility due to adsorption of sodium ions at the carbonyl groups of the lipids, in agreement with experiments indicating that the presence of NaCl renders the electrophoretic mobility of POPC vesicles more positive. Our findings argue against several theoretical assumptions for this system. First, we find that the surface is not sharply defined but that the water density shows a smooth transition over a length scale of 1 nm which, here, is comparable to the Debye screening length and, hence, to the thickness of the double layer. Second, the molecular shear plane resides in the headgroup region where continuum hydrodynamics is not applicable. Third, the effective viscosity in this region is found to be 2-fold higher than in the bulk liquid. Fourth, the zeta potential evaluated at the molecular scale is dominated by the dipole potential. Due to the dominance of the dipole potential, the molecular zeta potential is an order of magnitude larger than the zeta potential from the continuum theory.

Our results might have widespread implications for interpretation of electrokinetic studies in general. We have demonstrated the importance of considering the increased viscosity of interfacial water and the dipole potential at the shear plane, in order to improve the current theory.

ASSOCIATED CONTENT

Supporting Information

The SPC model describes water at interfaces more accurately than the SPC/E model. This material is available free of charge via the Internet at http://pubs.acs.org.

AUTHOR INFORMATION

Corresponding Author

*E-mail: volker.knecht@physik.uni-freiburg.de.

Present Addresses

[†]Biomolecular Dynamics, Institute of Physics, Albert Ludwigs University, Hermann-Herder Straße 3, D-79104 Freiburg, Germany.

[‡]MELAG Medical Technology, Geneststraße 6−10, D-10829 Berlin, Germany.

Notes

The authors declare no competing financial interest.

ACKNOWLEDGMENTS

V.K. thanks O. Velev and M.L. Berkowitz for useful discussions.

REFERENCES

(1) Reuss, F. Notice sur un nouvel effet de l'électricité galvanique. *Mémoires de la Société Imperiale des Naturalistes de Moscou* **1809**, *2*, 327−336.

(2) von Helmholtz, H. Studien über electrische Grenzschichten. *Ann. Phys. Chem.* **1979**, *243*, 337− 382.

(3) von Smoluchowski, M. Elektrische Endosmose und Strömungsströme. Handbuch der Elektrizität und des Magnetismus. *Leipzig* **1921**, 366−428.

(4) Hunter, R. J. *Zeta Potential in Colloid Science*; Academic Press: San Diego, 1981.

(5) Booth, F. Theory of electrokinetic effects. *Nature* **1948**, *161*, 83−86.

(6) Semenikhin, N. M.; Dukhin, S. S. Calculation of electrophoretic mobility of a spherical particle, with account taken of polarization of a moderately thin double-layer. *Coll. J. USSR* **1975**, *37*, 1017−1022.

(7) O'Brien, R. W.; Hunter, R. J. The electrophoretic mobility of large colloidal particles. *Can. J. Chem.* **1981**, *59*, 1878−1887.

(8) Delgado, A. V.; Gonzalez-Caballero, F.; Hunter, R. J.; Koopal, L. K.; Lyklema, J. Measurement and interpretation of electrokinetic phenomena. *J. Colloid Interface Sci.* **2007**, *309*, 194−224.

(9) Lyklema, J.; Rovillard, S.; De Coninck, J. Electrokinetics: The properties of the stagnant layer unraveled. *Langmuir* **1998**, *14*, 5659−5663.

(10) Böckmann, R. A.; Hac, A.; Heimburg, T.; Grubmüller, H. Effect of sodium chloride on a lipid bilayer. *Biophys. J.* **2003**, *85*, 1647−1655.

(11) Vacha, R.; Horinek, D.; Berkowitz, M. L.; Jungwirth, P. Hydronium and hydroxide at the interface between water and hydrophobic media. *Phys. Chem. Chem. Phys.* **2008**, *10*, 4975−4980.

(12) Eisenberg, M.; Gresalfi, T.; Riccio, T.; McLaughlin, S. Adsorption of mono-valent cations to bilayer membranes containing negative phospholipids. *Biochemistry* **1979**, *18*, 5213−5223.

(13) Klasczyk, B.; Knecht, V.; Lipowsky, R.; Dimova, R. Interactions of alkali metal chlorides with phosphatidylcholine vesicles. *Langmuir* **2010**, *26*, 18951−18958.

(14) Binder, H.; Zschornig, O. The effect of metal cations on the phase behavior and hydration characteristics of phospholipid membranes. *Chem. Phys. Lipids* **2002**, *115*, 39−61.

(15) Pabst, G.; Hodzic, A.; Strancar, J.; Danner, S.; Rappolt, M.; Laggner, P. Rigidification of neutral lipid bilayers in the presence of salts. *Biophys. J.* **2007**, *93*, 2688−2696.

(16) Berkowitz, M. L.; Vacha, R. Aqueous solutions at the interface with phospholipid bilayers. *Acc. Chem. Res.* **2012**, *45*, 74−82.

(17) Cordomí, A.; Edholm, O.; Perez, J. J. Effect of ions on a dipalmitoyl phosphatidylcholine bilayer. A molecular dynamics simulation study. *J. Phys. Chem. B* **2008**, *112*, 1397−1408.

(18) Gurtovenko, A. A.; Vattulainen, I. Effect of NaCl and KCl on phosphatidylcholine and phosphatidylethanolamine lipid membranes: Insight from atomic-scale simulations for understanding salt-induced effects in the plasma membrane. *J. Phys. Chem. B* **2008**, *112*, 1953.

(19) Klasczyk, B.; Knecht, V. Validating affinities for ion-lipid association from simulation against experiment. *J. Phys. Chem. A* **2011**, *115*, 10587−10595.

(20) Pandit, S. A.; Bostick, D.; Berkowitz, M. L. Molecular dynamics simulation of a dipalmitoylphosphatidylcholine bilayer with NaCl. *Biophys. J.* **2003**, *84*, 3743−3750.

(21) Vacha, R.; Berkowitz, M. L.; Jungwirth, P. Molecular model of a cell plasma membrane with an asymmetric multicomponent composition: Water permeation and ion effects. *Biophys. J.* **2009**, *96*, 4493−4501.

(22) Vácha, R.; Jurkiewicz, P.; Petrov, M.; Berkowitz, M. L.; Böckmann, R. A.; Barucha- Kraszewska, J.; Hof, M.; Jungwirth, P. Mechanism of interaction of monovalent ions with phosphatidylcholine lipid membranes. *J. Phys. Chem. B* **2010**, *114*, 9504−9509.

(23) Vácha, R.; Siu, S. W. I.; Petrov, M.; Böckmann, R. A.; Barucha-Kraszewska, J.; Jurkiewicz, P.; Hof, M.; Berkowitz, M. L.; Jungwirth, P. Effects of alkali cations and halide anions on the DOPC lipid membrane. *J. Phys. Chem. A* **2009**, *113*, 7235−7243.
(24) Gurtovenko, A. A. Asymmetry of lipid bilayers induced by monovalent salt: Atomistic molecular-dynamics study. *J. Chem. Phys.* **2005**, *122*, 244902.
(25) Porasso, R. D.; Lopez Cascales, J. J. Study of the effect of Na^+ and Ca^{2+} ion concentration on the structure of an asymmetric DPPC/DPPC plus DPPS lipid bilayer by molecular dynamics simulation. *Colloids Surf., B* **2009**, *73*, 42−50.
(26) Valley, C. C.; Perlmutter, J. D.; Braun, A. R.; Sachs, J. N. NaCl interactions with phosphatidylcholine bilayers do not alter membrane structure but induce long-range ordering of ions and water. *J. Membr. Biol.* **2011**, *244*, 35−42.
(27) Martin-Molina, A.; Rodriguez-Beas, C.; Faraudo, J. Effect of calcium and magnesium on phosphatidylserine membranes: Experiments and all-atomic simulations. *Biophys. J.* **2012**, *102*, 2095−2103.
(28) Vácha, R.; Marsalek, O.; Willard, A. P.; Bonthuis, D. J.; Netz, R. R.; Jungwirth, P. Charge transfer between water molecules as the possible origin of the observed charging at the surface of pure water. *J. Phys. Chem. Lett.* **2012**, *3*, 107−111.
(29) Yeh, I. C.; Berkowitz, M. L. Dielectric constant of water at high electric fields: Molecular dynamics study. *J. Chem. Phys.* **1999**, *110*, 7935−7942.
(30) Berger, O.; Edholm, O.; Jähnig, F. Molecular dynamics simulations of a fluid bilayer of dipalmitoylphosphatidylcholine at full hydration, constant pressure, and constant temperature. *Biophys. J.* **1997**, *72*, 2002−2013.
(31) van Gunsteren, W. F.; Berendsen, H. J. C. *Groningen Molecular Simulation (GROMOS) Library Manual*; BIOMOS: Groningen, The Netherlands; 1987.
(32) Berendsen, H. J. C.; Postma, J. P. M.; van Gunsteren, W. F.; Hermans, J. In *Intermolecular Forces*; Pullman, B., Ed.; D. Reidel Publishing Company: Dordrecht, 1981; pp 331−342.
(33) Miyamoto, S.; Kollman, P. A. SETTLE: An analytical version of the SHAKE and RATTLE algorithm for rigid water models. *J. Comput. Chem.* **1992**, *13*, 952−962.
(34) Hess, B.; Bekker, H.; Berendsen, H. J. C.; Fraaije, J. G. E. M. LINCS: A Linear Constraint Solver for Molecular Simulations. *J. Comput. Chem.* **1997**, *18*, 1463−1472.
(35) Berendsen, H. J. C.; Postma, J. P. M.; van Gunsteren, W. F.; DiNola, A.; Haak, J. R. Molecular dynamics with coupling to an external bath. *J. Chem. Phys.* **1984**, *81*, 3684.
(36) Bonthuis, D. J.; Horinek, D.; Bocquet, L.; Netz, R. R. Electrohydraulic power conversion in planar nanochannels. *Phys. Rev. Lett.* **2009**, *103*, 144503.
(37) Darden, T.; York, D.; Pedersen, L. Particle mesh Ewald: An N·log (N) method for Ewald sums in large systems. *J. Chem. Phys.* **1993**, *98*, 10089.
(38) van der Spoel, D.; Lindahl, E.; Hess, B.; Groenhof, G.; Mark, A. E.; Berendsen, H. J. C. GROMACS: Fast, flexible, and free. *J. Comput. Chem.* **2005**, *26*, 1701−1718.
(39) Knecht, V.; Risselada, H. J.; Mark, A. E.; Marrink, S. J. Electrophoretic mobility does not always reflect the charge on an oil droplet. *J. Colloid Interface Sci.* **2008**, *318*, 477−486.
(40) Neumann, M. Dipole-moment fluctuation formulas in computer simulations of polar systems. *Mol. Phys.* **1983**, *50*, 841−858.
(41) Heinz, T. N.; van Gunsteren, W. F.; Hünenberger, P. H. Comparison of four methods to compute the dielectric permittivity of liquids from molecular dynamics simulations. *J. Chem. Phys.* **2001**, *115*, 1125−1136.
(42) Kastenholz, M. A.; Hünenberger, P. H. Computation of methodology-independent ionic solvation free energies from molecular simulations. I. The electrostatic potential in molecular liquids. *J. Chem. Phys.* **2006**, *124*, 124106.
(43) Zhou, Y.; Raphael, R. M. Solution pH alters mechanical and electrical properties of phosphatidylcholine membranes: Relation between interfacial electrostatics, intramembrane potential, and bending elasticity. *Biophys. J.* **2007**, *92*, 2451−2462.
(44) Yeh, I. C.; Hummer, G. Diffusion and electrophoretic mobility of single-stranded RNA from molecular dynamics simulations. *Biophys. J.* **2004**, *86*, 681−689.
(45) Marinova, K. G.; Alargova, R. G.; Denkov, N. D.; Velev, O. D.; Petsev, D. N.; Ivanov, I. B.; Borwankar, R. P. Charging of oil-water interfaces due to spontaneous adsorption of hydroxyl ions. *Langmuir* **1996**, *12*, 2045−2051.
(46) Frumin, L.; Peltek, S.; Zilberstein, G. Nonlinear electrophoresis and focusing of macromolecules. *J. Biochem. Biophys. Methods* **2001**, *48*, 269−282.
(47) Plenert, M. L.; Shear, J. B. Microsecond electrophoresis. *Proc. Natl. Acad. Sci. U.S.A.* **2003**, *100*, 3853−3857.
(48) Knecht, V.; Klasczyk, B. Specific binding of chloride ions to lipid vesicles and implications at molecular scale. *Biophys. J.* **2013**, *104*, 818−824.
(49) Smith, P. E.; van Gunsteren, W. F. The viscosity of SPC and SPC/E water at 277-K and 300-K. *Chem. Phys. Lett.* **1993**, *215*, 315−318.
(50) Hill, R. J. Hydrodynamics and electrokinetics of spherical liposomes with coatings of terminally anchored poly(ethylene glycol): Numerically exact electrokinetics with selfconsistent mean-field polymer. *Phys. Rev. E* **2004**, *70*, 051406.
(51) Wassall, S. R. Pulsed field-gradient-spin echo NMR studies of water diffusion in a phospholipid model membrane. *Biophys. J.* **1996**, *71*, 2724−2732.
(52) Rog, T.; Murzyn, K.; Pasenkiewicz-Gierula, M. The dynamics of water at the phospholipid bilayer surface: A molecular dynamics simulation study. *Chem. Phys. Lett.* **2002**, *352*, 323−327.
(53) van Buuren, A. R.; Marrink, S. J.; Berendsen, H. J. C. Characterization of aqueous interfaces with different hydrophobicities by molecular-dynamics. *Colloid Surf., A* **1995**, *102*, 143−157.
(54) Wilson, M. A.; Pohorille, A.; Pratt, L. R. Surface-potential of the water liquid vapor interface. *J. Chem. Phys.* **1988**, *88*, 3281−3285.
(55) Feller, S. E.; Pastor, R. W.; Rojnuckarin, A.; Bogusz, S.; Brooks, B. R. Effect of electrostatic force truncation on interfacial and transport properties of water. *J. Phys. Chem.* **1996**, *100*, 17011−17020.
(56) Marrink, S. J.; Marcelja, S. Potential of mean force computations of ions approaching a surface. *Langmuir* **2001**, *17*, 7929−7934.
(57) Stillinger, F. H.; Weber, T. A. Dynamics of structural transitions in liquids. *Phys. Rev. A* **1983**, *28*, 2408−2416.
(58) Croxton, C. A. Molecular-orientation and interfacial properties of liquid water. *Physica A* **1981**, *106*, 239−259.
(59) Tatulian, S. Binding of alkaline-earth metal-cations and some anions to phosphatidylcholine liposomes. *Eur. J. Biochem.* **1987**, *170*, 413−420.
(60) Winiski, A. P.; McLaughlin, A. C.; McDaniel, R. V.; Eisenberg, M.; McLaughlin, S. An experimental test of the discreteness-of-charge effect in positive and negative lipid bilayers. *Biochemistry* **1986**, *25*, 8206−8214.

Macro- versus microscopic view on the electrokinetics of a water/membrane interface: Supporting Information

Volker Knecht,[a] Benjamin Klasczyk,[b] Rumiana Dimova

Theory & Bio-Systems, Max Planck Institute of Colloids and Interfaces,

Science Park Golm, D-14424 Potsdam, Germany

E-mail:

[a] corresponding author, email to volker.knecht@physik.uni-freiburg.de; current address: Biomolecular Dynamics, Institute of Physics, Albert Ludwigs University, Hermann-Herder Straße 3, D-79104 Freiburg, Germany

[b] current address: MELAG Medical Technology, Geneststraße 6 – 10, D-10829 Berlin, Germany

Supplementary Methods

SPC model more accurately describes water at interfaces than SPC/E model

Both the SPC[1] and the SPC/E model[2] are parameterized such as to reproduce the density and heat of vaporization of water at ambient conditions. As they are nonpolarizable models the effect of the polarizability is implicitely taken into account by choosing an enhanced permanent dipole moment. The difference between the models is that in contrast to SPC the SPC/E model considers the polarization energy which leads to a larger permanent dipole moment and thereby better bulk properties. However, the polarization of the water depends on the environment and if the latter is less polar than in bulk water like in vapor or at a water/membrane interface, real water molecules are less polarized. In such environments, the SPC model with its lower permanent dipole moment appears to be more accurate than the SPC/E model.[3] For instance, the solubility of simulated

*To whom correspondence should be addressed

water in GROMOS decane for SPC water (4×10^{-5} mole fractions) is closer to the experimental value (10×10^{-5} mole fractions) than that of SPC/E water (0.9×10^{-5} mole fractions) [4]. Furthermore, the hydrogen-bonding energy between two water moleculs in the dilute gas phase for SPC (-27.6 kJ/mol) is closer to the experimental value (-22.6 kJ/mol) and the estimate from *ab initio* calculations (-21.0 kJ/mol) than the value for SPC/E (-30.1 kJ/mol). The second virial coefficents show similar trends.[5] Thus, recent versions of the GROMOS force field for proteins were optimized to reproduce hydration free energies in conjunction with the SPC model for the water.[6]

References

1. Berendsen, H. J. C.; Postma, J. P. M.; van Gunsteren, W. F.; Hermans, J. Interaction Models for Water in Relation to Protein Hydration. In *Intermolecular Forces*; Pullman, B., Ed.; D. Reidel Publishing Company: Dordrecht, 1981; pp 331–342.

2. Berendsen, H. J. C.; Grigera, J. R.; Straatsma, T. P. *J. Phys. Chem.* **1987**, *91*, 6269–6271.

3. Klasczyk, B.; Knecht, V. *J. Chem. Phys.* **2010**, *132*, year.

4. van Buuren, A. R.; Marrink, S. J.; Berendsen, H. J. C. *J. Phys. Chem.* **1993**, *97*, 9206–9212.

5. Berendsen, H. J. C. *Simulating the Physical World – Hierarchical Modeling from Quantum Mechanics to Fluid Dynamics*, 1st ed.; Cambridge University Press: Cambridge, UK, 2007.

6. Oostenbrink, C.; Villa, A.; Mark, A.; Van Gunsteren, W. *J. Comput. Chem.* **2004**, *25*, 1656–1676.